POLITECNICO DI TORINO
Repository ISTITUZIONALE

Performance optimization in ultra-long Raman laser amplified 10x30 GBaud DP-QPSK transmission: Balancing RIN and ASE noise

(Article begins on next page)

18 April 2024

Check for updates

Performance optimization in ultra-long Raman laser amplified 10x30 GBaud DP-QPSK transmission: balancing RIN and ASE noise

Francesca Gallazzi,[1,*] Giuseppe Rizzelli,[1] Md Asif Iqbal,[2] Mingming Tan,[2] Paul Harper,[2] and Juan Diego Ania-Castañón[1]

[1]*Instituto de Óptica "Daza de Valdés", IO-CSIC, C/Serrano 121, 28006, Madrid, Spain*
[2]*AIPT, Aston University, Birmingham B4 7ET, UK*
[*]francesca.gallazzi@io.cfmac.csic.es

Abstract: We experimentally evaluate the influence of RIN transfer from pump to signal on the transmission performance of a 10 x 30 Gbaud DP-QPSK transmission system using a 2nd-order ultra-long Raman fiber laser amplifier, considering the effect of cavity front-end reflectivity and forward pump power ratio. The evolution of the Q-factors with distance up to maximum reach is monitored for a 10 x 30 Gbaud DP-QPSK transmission system with WDM channels between 1542.94 nm to 1550.12 nm. A maximum transmission distance of 6479 km is found for configurations with low forward pump powers corresponding to the optimal balance between RIN and ASE impairments.

References and links

1. I. Nasieva, J.D. Ania-Castañón, and S. K. Turitsyn, "Nonlinearity management in fibre links with distributed amplification," Electron. Lett. **39**(11), 856–857 (2003).
2. W. S. Pelouch, "Raman amplification: an enabling technology for long-haul coherent transmission systems," J. Lightwave Technol. **34**(1), 6–19 (2016).
3. J. D. Ania-Castañón, "Quasi-lossless transmission using second-order Raman amplification and fiber Bragg gratings," Opt. Express **12**(19), 4372–4377 (2004).
4. J. D. Ania-Castañón, T. J. Ellingham, R. Ibbotson, X. Chen, L. Zhang, and S. K. Turitsyn, "Ultralong Raman fiber lasers as virtually lossless optical media," Phys. Rev. Lett. **96**(2), 023902 (2006).
5. P. Rosa, J.D. Ania-Castañón, P. Harper, "Unrepeated DPSK transmission over 360 km SMF-28 fibre using URFL based amplification," Opt. Express **22**(8), 9687–9692 (2014).
6. M. Tan, P. Rosa, S. T. Le, I. D. Phillips, P. Harper, "Evaluation of 100G DP-QPSK long-haul transmission performance using second order co-pumped Raman laser based amplification," Opt. Express **23**(17), 22181–22189 (2015).
7. L. Galdino, M. Tan, D. Lavery, P. Rosa, R. Maher, I. D. Phillips, J. D. Ania-Castañón, P. Harper, R. I. Killey, B. C. Thomsen, S. Makovejs, and P. Bayvel, "Unrepeated Nyquist PDM-16QAM transmission over 364 km using Raman amplification and multi-channel digital back-propagation," Opt. Lett. **40**(13), 3025–3028 (2015).
8. I. Phillips, M. Tan, M. F. Stephens, M. E. McCarthy, E. Giacoumidis, S. Sygletos, P. Rosa, S. Fabbri, S. T. Le, T. Kanesan, S. K. Turitsyn, N. J. Doran, P. Harper, A. D. Ellis, "Exceeding the nonlinear-Shannon limit using Raman laser based amplification and optical phase conjugation," in *Optical Fiber Communication conference*, OSA Technical Digest (online) (Optical Society of America, 2014), paper M3C.1.
9. C. R. S. Fludger, V. Handerek, R. J. Mears, "Pump to signal RIN transfer in Raman fiber amplifiers," J. Lightwave Technol. **19**(8), 1140–1148 (2001).
10. B. Bristiel, S. Jiang, P. Gallion, and E. Pincemin, "New model of noise figure and RIN transfer in fiber Raman amplifiers," IEEE Photonics Technol. Lett. **18**(8), 980–982 (2006).
11. M. Alcón-Camas, J. D. Ania-Castañón, "RIN transfer in 2nd-order distributed amplification with ultralong fiber laser," Opt. Express **18**(23), 23569-–23575 (2010).
12. J. Nuño, M. Alcon-Camas, J.D. Ania-Castañón, "RIN transfer in random distributed feedback fiber lasers," Opt. Express **20**(24), 27376–27381 (2012).
13. G. Rizzelli, M. A. Iqbal, F. Gallazzi, P. Rosa, M. Tan, J. D. Ania-Castañón, L. Krzczanowicz, P. Corredera, I. Phillips, W. Forysiak, P. Harper, "Impact of input FBG reflectivity and forward pump power on RIN transfer in ultralong Raman laser amplifiers," Opt. Express **24**(25), 29170–29175 (2016).

14. M. Tan, P. Rosa, S. T. Le, M. A. Iqbal, I. D. Phillips, P. Harper, "Transmission performance improvement using random DFB laser based Raman amplification and bidirectional second-order pumping," Opt. Express **24**(3), 2215–2221 (2016).
15. L. Barker, A. E. El-Taher, M. Alcón-Camas, J. D. Ania-Castañón, P. Harper, "Extended bandwidth for long haul DWDM transmission using ultra-long Raman fiber lasers," in *Proc. of ECOC 2010*, Torino, P4.14 (1–3) (2010).

1. Introduction

When compared to traditional EDFA lumped amplification, distributed Raman amplification presents a number of well-known potential benefits arising from its improved balance between noise and nonlinear impairments [1, 2]. In particular, high-order Raman amplification using ultra-long Raman fiber lasers (URFLs) [3, 4] has proven to be a promising solution for future long-haul and unrepeatered communication links, combining a simple design with low signal power variation and superior optical signal to noise ratios (OSNRs) [5, 6]. Moreover, URFLs have displayed excellent results when paired with different nonlinear mitigation techniques, be it digital, such as digital backpropagation (DBP) [7], or physical, such as mid-link optical phase conjugation (OPC) [8]. Unfortunately, the ultimate performance of URFL amplifiers is limited by relative intensity noise (RIN) transfer from pump to signal, due to the fact that, through the fast process of Raman amplification, oscillations on the pump intensity are passed onto the signal. This effect is maximised for co-propagating pumps, due to the superposition of the pump and signal during transmission [9,10]. URFLs rely on cascaded pumping to efficiently distribute the gain along the transmission link. This is achieved by transforming the transmission spans into ultra-long active cavities lasing at the first Stokes frequency of the pump. Two fiber Bragg gratings (FBGs), typically with high-reflectivities, delimit the cavity, improving pump-to-Stokes conversion efficiency and back-reflecting Stokes radiation into the cavity for better gain distribution. In a low-depletion regime, symmetric pumping leads to the lowest signal power variation (SPV) along the span, and hence to the best possible balance between ASE noise and nonlinear impairments. Unfortunately, high forward pump powers, necessary to maintain symmetry in long spans or when amplifying a high number of channels, may be detrimental for transmission performance, as it is directly related to an increased RIN transfer from the pump to the propagating signal [3, 11–13]. In order to overcome the problem of RIN transfer, the use of Raman amplification based on certain configurations of ultralong random distributed feedback (DFB) fiber lasers has been recently proposed and successfully demonstrated in coherent transmission schemes. In such lasers, the FBG at the beginning of the cavity is removed, leaving a half open cavity which reduces front-end backreflections to zero, with the downside of reduced forward (FW) pump efficiency [14].

In a recent work [13] it is shown experimentally and numerically how, in a 2nd-order Raman amplifier similar to the one tested in the present study, RIN transfer increases with increasing reflectivity at the front end of the cavity, as well as with forward pump powers (reaching a saturation level over 50% of FW pump power ratio). Building upon this previous work on RIN characterization in URFL systems [13], we evaluate here the direct impact of RIN on transmission performance, using a 30 GBaud dual polarization quadrature phase shift keying (DP-QPSK) system transmitting 10 WDM signal channels in the C-band, using a cavity in which it is possible to vary both front-end FBG reflectivity and pump power split in order to control RIN transfer in the URFL amplification scheme. We tested different configurations of front-FBG reflectivity and pump power ratio adjusting the amplifier through the variable optical attenuators located at the pump outputs and in the variable reflectivity module at the front end of the cavity.

2.   Experimental set-up

Figure 1(a) depicts the set-up of the 2nd-order ultra-long Raman laser amplifier tested in the present work. It is built with 108 km of standard single mode fiber (SSMF) pumped bidirectionally by two equal highly depolarized Raman fiber laser operating at 1366 nm, acting as second order pumps. The basic cavity is enclosed by two FBGs, centered at 1454 nm corresponding to the pump's first Stokes wavelength. Two wavelength division multiplexers (WDM) are employed to couple and split pumps, signals and first Stokes wavelengths at the two sides of the cavity. The FBG at the end of the cavity presents a high (> 95%) fixed reflectivity at its central wavelength (1454 nm), whereas the front-end reflector is actually a variable reflectivity module (VRM), combining a high-reflectivity FBG (> 95%) and a variable optical attenuator (VOA), which allows testing of the cavity performance over a continuum of FBG reflectivities, controlling the amount of backreflections into the cavity. Back-to-back 99%-1% splitters inside the cavity allow for the real-time monitoring of the VRM reflectivity. Due to the insertion losses caused by the taps, variable attenuator and WDM, the maximum effective reflectivity achievable with the VRM is 20%. Other two VOAs are located at the pumps' output to adjust the pump powers, in order to keep pump RIN fixed and independent from pump power. The pumps are, thus, set to the maximum power needed, which is then attenuated to obtain the necessary pump split for each measurement.
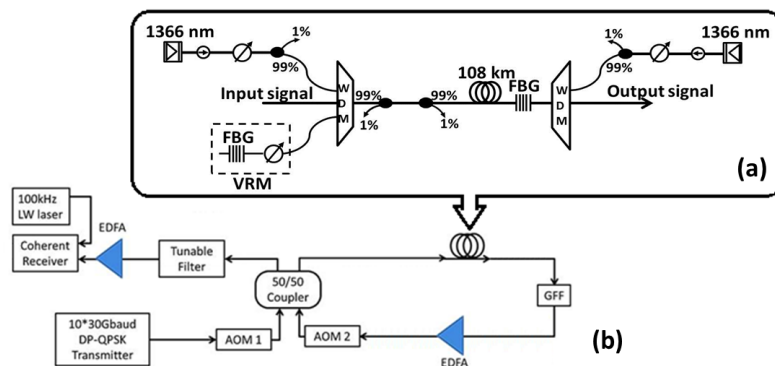

Fig. 1. Set-up of the 2nd-order ultra-long Raman amplifier (a) and the 10x30 GBaud DP-QPSK transmission system (b).

In order to monitor transmission performance, different URFL configurations are employed to fully compensate for the Raman span and passive component losses in a 10 x 30 GBaud coherent detection DP-QPSK transmission system, as shown in Fig. 1(b). In this set-up, the 108 km transmission span is included in a recirculating loop. The transmitter comprises ten 100 GHz spaced distributed feedback lasers located between 1542.94 nm and 1550.12 nm. In order to test each available channel, the grid is combined with a 100 kHz linewidth tunable laser that replaces the corresponding DFB laser during the measurement cycle. In each channel, the multiplexed signals were QPSK modulated with normal and inverse 2^{31} -1 PRBS patterns at 30 Gb/s with a relative delay between I (in-phase) and Q (quadrature) of 18 bits. The PolMux was implemented with a delay of 300 bits between the two polarisation states. The total transmission rate was 10 x 120 Gb/s. No temporal decorrelation is applied to the data transmitted at each wavelength, but fiber dispersion effectively decorrelates the 10 WDM channels temporally. The modulated DP-QPSK signals are launched into the previously described transmission span in the recirculating loop. The output spectrum is equalized by a gain flattening filter (GFF) and an EDFA compensates for the losses of the loop before the coherent receiver. A detailed description of a similar system is available in [6]. The resultant traces are post-processed off-line with

digital signal processing (DSP). Finally, the Q-factors are calculated from measured bit error rates (BERs), averaged over two million bits.

3. Results and discussion

Different configurations of the URFL cavity are tested to investigate their transmission performances, considering the impact that RIN transfer may have on them. Q-factors have been obtained for front-end FBG reflectivities of 1.5% (obtained with a flat-end PC connector substituting the VRM), 10% and 20% and forward pump power ratios of 10%, 20% and 40%. Q-factors for 0% (backward pumping only) FW pump power ratio have been measured only for the case of 20% front-end reflectivity without loss of generality, since, as previously shown in [14], the performance is not altered in this case by variations in front-end FBG reflectivity. Please note that, unlike the FBG reflector, which acts as a sharp filter around the Stokes wavelength, the flat-end connector (giving a 1.5% reflectivity) reflects all wavelengths equally, including the pump ones.
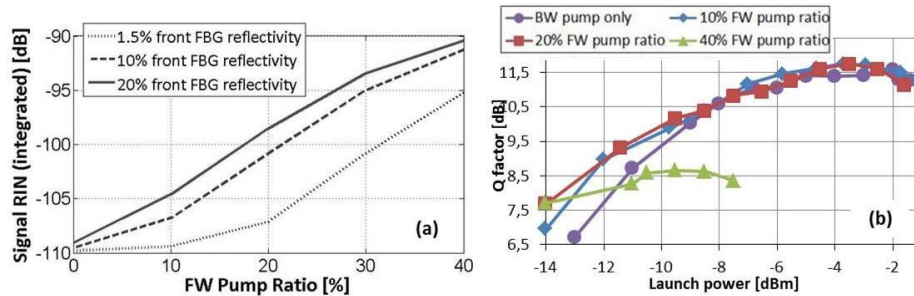

Fig. 2. Simulated signal RIN integrated over 1 MHz as a function of FW pump power ratio and front-FBG reflectivity (a). Launch power versus Q-factors at 2159 km, measured at 1545.32 nm for 20% front-FBG reflectivity (b).

Figure 2(a) shows the simulated signal RIN, integrated over 1 MHz, obtained from the calculated RIN transfer function for each of the investigated cases, taking as input the measured pump RIN. From the figure it is clear how RIN increases both with FW pump ratio and front-FBG reflectivity. Figure 2(b) shows the variation of the Q-factors of the measured channel at 1545.32 nm versus signal launch power at different forward pump power ratios maintaining a 20% front-FBG reflectivity and a fix transmission distance of 2159 km in the recirculating loop. Optimal signal launch powers are between -2 dBm and -4 dBm for FW pump ratios up to 20% of total pump power, while they shift down to between -8 dBm and -9 dBm for a FW pump ratio of 40%. This reduction in the optimal signal power is typical of quasi-lossless URFL amplification, and thus to be expected as gain becomes more evenly distributed as we approach to equal bidirectional pumping [15]. Please note that 40% FW pump ratio is the highest for which it was possible to achieve a BER below the forward error correction (FEC) threshold (corresponding to Q-factors above 8.5 dB). This is in line with the build-up of the RIN in the cavity, which can be expected to hinder the transmission performance.

Figures 3(a), 3(b) and 3(c) show the achievable Q-factors of the channel at 1545.32 nm as a function of transmission distance for the different cavity configurations. A maximum reach of 5399 km is achievable for the 1.5% flat-end connector -Fig. 3(a)- with 10% and 20% FW pump ratios (the second one giving the best results), but RIN transfer at 40% FW ratio quickly degrades performance despite the improved OSNR offered by the URFL configuration. The flat connector configuration offers, in any case, worse performance than any of the FBG-based configurations tested, possibly due to its extended reflection bandwidth. For a 10% reflectivity
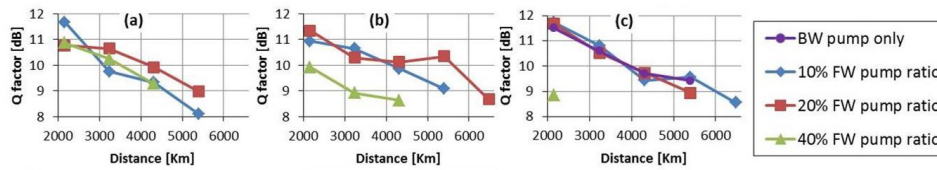
Fig. 3. Transmission distance versus Q-factors measured at 1545.32 nm for 1.5% (a), 10% (b) and 20% (c) front-end reflectivity.

front-FBG -Fig. 3(b)-, reach is extended to 6479 km for a 20% FW pump ratio, which offers the best trade-off between OSNR and RIN performance. The 20% reflectivity front-FBG -Fig. 3(c)- case can offer a similar reach of 6479 km (with better pump conversion efficiency) for a 10% FW pump ratio, but the performance is degraded for higher FW pump ratios due to RIN transfer, as well as for the backward-only pump case, in which ASE dominates. Regarding the results obtained with 40% FW pump ratio, it is clear that, besides allowing for shorter reaches (down to only 2159 km for 20% front-end reflectivity), the starting performance itself is worse than in the cases with lower FW pump ratios (which allow for Q-factors close to or over 11 dB at a 2159 km distance) and decreasing for higher front-FBG reflectivities.
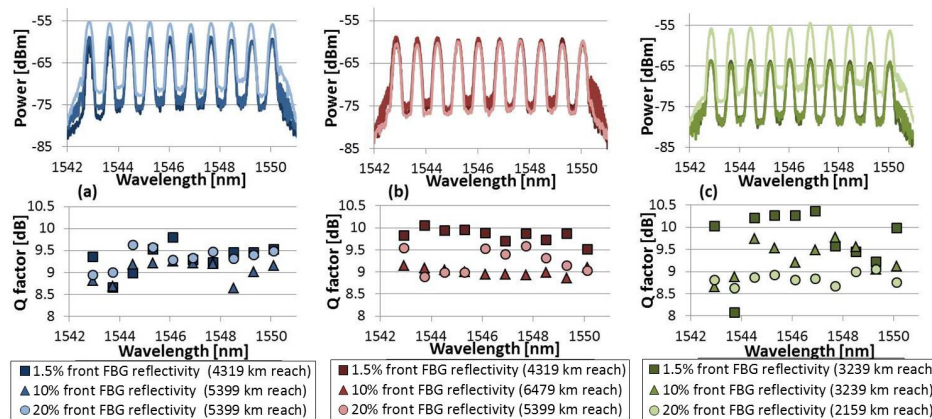

Fig. 4. Measured spectra and Q-factors at maximum reach of the 10 channels for 10% (a), 20% (b) and 40% (c) FW pump ratio.

Figure 4 displays the measured optical spectra and the Q-factors of the 10 WDM channels at maximum worst-channel attainable reach after FEC. As seen above, 10% and 20% FW pump ratios allow for "sweet spot" configurations in which OSNR and RIN impairments are balanced, which lead to reaches of at least 5399 km for the 10 channels, with good gain flatness resulting in a variation of less than 0.7 dB between the Q-factors of the different channels, except, as it may be expected, in the case of the flat connector (1.5%), in which performance is limited to 4319 km. The best performance is obtained for the case of 10% reflectivity and 20% FW pump power, with a 6479 km reach for all channels, with a Q-factors maximum variation between channels of 0.28 dB. Performance for the 40% FW pump ratio is poor for all cases, and down to 2159 km for the 20% front-FBG reflectivity, with higher variability between channels Q-factors.

As mentioned in section 2, the measurements are performed with fixed high output pump powers, which each time are attenuated by means of the variable optical attenuators located at the lasers outputs to obtain the necessary pump power ratio. Since pump RIN is dependent
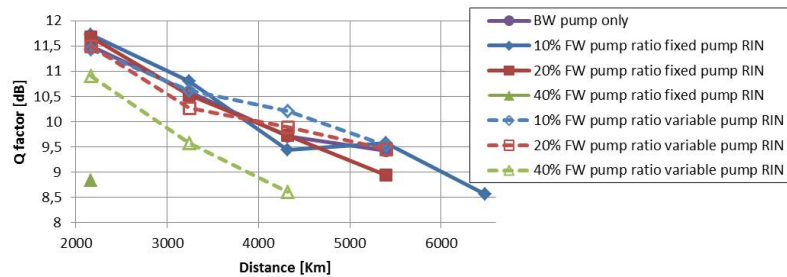
Fig. 5. Comparison fixed (solid) and variable (dashed) pump RIN: transmission distance versus Q-factors measured at 1545.32 nm for 20% front-end reflectivity.

on pump power, controlling the ouput pump power as mentioned above, the pump RIN is kept fixed and it is possible to eliminate its dependence from the power variation of the pumps. It is, thus, possible to isolate the effect of RIN transfer, taking into account that the pump always delivers the same RIN. Since we wanted to check the impact of RIN transfer on transmission performance, we performed the measurements with the described method. It is worth to mention though, as it has been shown in [10], that the signal RIN increases differently compared to what is presented in Fig. 2(a) when changing directly the pumps power in respect with the fixed pump RIN approach. In particular, for high front-end reflectivity of the cavity and high FW pump power ratio, the signal RIN is higher in the case of fixed pump RIN. We verify here this behavior on the transmission performance, presented in Fig. 5, where the Q-factors as function of transmission distance in a cavity with 20% front-end reflectivity are compared for the cases of fixed and variable pump RIN. While for low FW pump ratios they show comparable performances, it is clear that, increasing the FW pump to 40%, the set-up with variable RIN offers better performances incrementing the maximum reach from 2159 km of the fixed pump RIN case up to 4319 km.

4. Conclusions

We have evaluated the impact of front-FBG reflectivity and pump split on long-haul URFL-amplified systems performance. For the considered span length we can conclude that forward pump ratios above 20% with noisy fiber laser pumps should be avoided in general in combination with any kind of front-FBG reflector for the Stokes component, but the use of lower pump ratios can offer ASE noise reduction without compromising system performance because of RIN. Using a flexible variable reflectivity module and fixed-RIN fiber laser pumps, we have demonstrated the possibility of optimizing amplifier design to offer the best balance between ASE and RIN impairments for a 10 x 30 Gbaud DP-QPSK transmission system tested through a recirculating loop. For a 108 km ultra-long Raman laser amplifier, a 20% forward pump power ratio and 10% front-FBG reflectivity offered the best performance, allowing us to reach transmission distances of 6479 km for all the 10 channels between 1542.94 nm and 1550.12 nm. This optimal balance can be expected to be dependent on both transmission format and pump RIN specifications.